Zirconium-Catalyzed Amine Oxidation: A Mechanistic Study

Werner R. Thiel*[a] and Karsten Krohn[b]

Abstract: The zirconium-catalyzed oxidation of amines in the presence of hydroperoxides gives the corresponding nitro compounds in high yields. In the present paper, we describe mechanistic details of this three-step oxidation, which was investigated by means of DFT calculations. It is shown that *N*-oxides, hydroxylamines, and nitroso derivatives are formed as intermediates. These compounds had already been postulated on the basis of synthetic experiments. During the oxidation process, the nitrogen atom changes its electronic character from a strong nucleophilic center to a moderate electrophilic center; this is reflected by the geometry of the transition states of the oxygen-transfer process.

Keywords: amines · catalytic oxidations · density function calculations · reaction mechanisms · zirconium

Introduction

The oxidation of phenols, alcohols, and amines with *tert*-butyl hydroperoxide in the presence of transition-metal alkoxide catalysts has been the subject of intense investigations during the last years.[1] Particularly primary amines are oxidized to the corresponding nitro compounds with high yields and high selectivities, by reaction with a combination of $[Zr(OtBu)_4]$ (catalyst) and *t*BuOOH (oxidizing agent).

The oxidation of amines to nitro compound requires the transfer of three oxygen atoms per nitrogen atom ($RNH_2 + 3\,tBuOOH \rightarrow RNO_2 + 3\,tBuOH + H_2O$). It makes sense to assume that there are three steps of oxygen transfer and, therefore, at least two intermediates. This stepwise oxygen transfer was investigated in a series of experiments on the oxidation of primary *aromatic* amines **A** (Scheme 1; $x = 0$: R = aryl).[2, 3]

The presence of hydroxylamines **B** as intermediates in the oxidation of aromatic amines was proved indirectly by the isolation of azoxy compounds, which were formed in a coupling reaction with the nitroso compounds **C**. Aromatic nitroso compounds **C** were isolated in up to 50 % yields when donor-substituted anilines were used as substrates. In kinetic competition experiments with 4-methoxyaniline, aniline, and

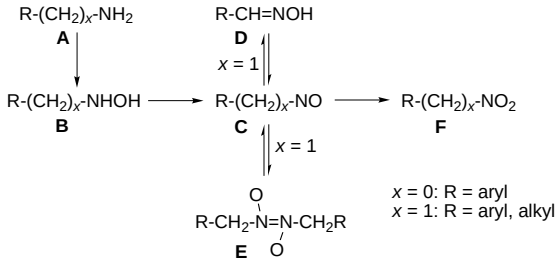

Scheme 1.

4-nitroaniline, the formation of 1,4-dinitrobenzene was observed from the very beginning, while 4-methoxy-1-nitrobenzene could be detected only after an induction period of ≈ 30 min. Here, the first two oxygen-transfer reactions were rapid and the last, which oxidized 4-methoxy-1-nitrosobenzene to 4-methoxy-1-nitrobenzene, was slow. This can be explained with a fundamental change of the electronic situation of the nitrogen atom with the progressive oxidation: while amines and hydroxylamines act as *nucleophiles*, the nitroso derivatives are *electrophiles*. Owing to its oxenoid character, *t*BuOOH, activated by a transition metal center, can follow these changes in electronic nature of the substrates.

Different side reactions may occur during the oxidation of *aliphatic* amines (Scheme 1; $x = 1$: R = alkyl, aryl):[4] the nitroso compounds **C** can tautomerize to the corresponding oximes **D** or undergo a dimerization to give **E**.[3] Incomplete oxidation was sometimes observed in the reaction with MCPBA; this was caused by the formation of the nitroso dimers **E**.[5] In contrast, when $[Zr(OtBu)_4]$ and *t*BuOOH are applied, no intermediates can be isolated, and the yields of aliphatic nitro compounds **F** are high. The only exceptions are benzylic amines, in which the resulting C–H acidic benzylic

[a] Prof. Dr. W. R. Thiel
Institut für Chemie, TU Chemnitz
Strasse der Nationen 62, 09111 Chemnitz (Germany)
Fax: (+49) 371-531-1833
E-mail: werner.thiel@chemie.tu-chemnitz.de

[b] Prof. Dr. K. Krohn
FB13—Chemie und Chemietechnik, Universität Paderborn
Warburger Str. 100, 33098 Paderborn (Germany)
Fax: (+49) 5251-60-3245
E-mail: kk@chemie.uni-paderborn.de

  0947-6539/02/0805-1049 $ 17.50+.50/0

nitro compounds are partly cleaved to give the corresponding aldehydes.[6] C=N bonds of hydrazones can also be cleaved oxidatively in good yields.[6] Even secondary mixed aliphatic–aromatic amines can be oxygenated to the corresponding nitro compounds;[7] in this case, a C–N bond has to be broken. Nitrones were postulated as the intermediates. While a whole series of experiments has been undertaken to get a deeper insight into this cascade oxidation reaction, nothing is known up to now about the nature of the transition states of the oxygen transfers.

On the other hand, detailed mechanistic studies on the epoxidation of allylic alcohols with titanium catalysts and of unfunctionalized olefins with molybdenum–peroxo complexes were carried out in the last years.[8, 9] Here, the activation of the oxidizing agent (e.g., *t*BuOOH) commences with a ligand-exchange reaction, which leads to an η^2 coordination of the resulting *t*BuOO$^-$ ligand (Scheme 2).

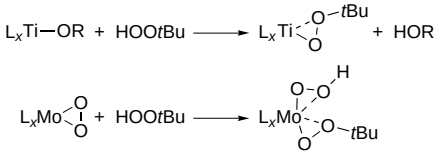

Scheme 2.

It can be taken as a working hypothesis that the activation of hydroperoxides at zirconium alcoholates should follow the same principle. Additionally, it is known that, among all zirconium–alcoholato complexes, [Zr(O*t*Bu)$_4$] is by far the best catalyst for the oxidation of amines to the corresponding nitro derivatives with *t*BuOOH.[1] Its high activity was explained by the steric demand of the *tert*-butanolato ligands, which prevent this zirconium complex from undergoing nucleation. The zirconium alcoholates of secondary and primary alcohols have been found to be di- or oligonuclear compounds, with the metal centers bridged by alcoholato ligands. This feature reduces the Lewis acidity of the zirconium centers and their accessibility for the substrates, and, therefore, the activity of the oxidation system. The X-ray structure analysis of [Zr(O*t*Bu)$_4$] has not yet been published; however, the solid-state structure of the fluorinated compound [Zr{OC(CH$_3$)(CF$_3$)$_2$}$_4$] was recently investigated. A monomeric zirconium complex with a tetrahedrally coordinated metal center was found.[10] From the series of zirconium alkoxides with higher nucleation, [{Zr(O*i*Pr)$_3$(μ^2-O*i*Pr)(HO*i*Pr)}$_2$], [{Zr(O*i*Pr)$_2$(iso-eugenolato)(μ^2-O*i*Pr)}$_2$], and [{Zr(μ^2-O*t*Bu)(O*t*Bu)$_2$}$_3$(μ^3-O)(μ^3-O*t*Bu)] were structurally characterized.[11] The incorporation of a μ^3-bridging oxo ligand in the last compound is an indication of the sensitivity of zirconium alkoxides toward traces of water. This explains the use of molecular sieves during catalytic oxidations with these complexes.

Abstract in German: *Die zirkoniumkatalysierte Oxidation primärer Amine mit Hydroperoxiden liefert die entsprechenden Nitroverbindungen in hohen Ausbeuten. In der vorliegenden Arbeit wird der mehrstufige Reaktionsweg mithilfe von DFT-Rechnungen nachvollzogen. Es kann belegt werden, dass N-Oxide, Hydroxylamine und Nitrosoverbindungen als Intermediate auftreten. Diese Verbindungen wurden bereits früher bei Synthesen als Zwischenstufen beobachtet. Im Verlauf der Reaktion verändert das Stickstoffatom seinen elektronischen Charakter von einem starken nukleophilen hin zu einem moderat elektrophilen Zentrum. Dies zeigt sich deutlich in den Geometrien der Übergangszustände des Sauerstofftransfers.*

Results and Discussion

In the present paper, we report the results of quantum mechanical calculations on the primary amine/zirconium alcoholate/alkyl hydroperoxide system with a special focus on the nature of the catalytically active species and the changes in the electronic situation of the substrate during its oxidation. To keep the computing times acceptable, we used [Zr(OMe)$_4$] (**1a**) as the model catalyst, methyl amine as the substrate, and methyl hydroperoxide as the oxygen source for most of our calculations. Details of the quantum chemical calculations are summarized in the Experimental Section.

Ligand-exchange reactions in the system [Zr(OMe)$_4$] (1a) and MeOOH: Ligand exchange of OR by OOR ligands (Scheme 2) may give rise to the formation of mixed zirconium alcoholato/alkylperoxo complexes. Calculations on the series [Zr(OMe)$_x$(OOMe)$_{4-x}$] (**1a**–**e**; $x = 4-0$) resulted the optimized structures shown in Figure 1, which also presents the reaction enthalpies and structural details of **1a**–**e**.

The calculated bond lengths of **1a** are in good agreement with the structural data of terminal Zr–OR units obtained from the X-ray structure analysis of a series of zirconium alkoxo complexes (d(Zr–O)$_{obs}$: 1.90–1.95 Å).[10, 11] The experimental data were quite independent of the nuclearity of the complex. DFT calculations without additional polarization functions (see the Experimental Section) on nitrogen, oxygen, and carbon lead to much longer Zr–O distances.

The successive ligand exchange of OMe against OOMe ligands is exothermic with $\approx$2.2 kcal mol^{-1} for the series **1a** → **1b** → **1c** → **1d**. This is caused by an increasing stabilization of the Lewis-acidic metal center by an increasing number of η^2-coordinating OOMe ligands. However, the final ligand exchange reaction (**1d** → **1e**) was almost thermoneutral. The η^2 coordination of OOMe and, therefore, activation for oxygen transfer, is proved by short distances between the zirconium centers and the carbon-substituted oxygen atoms of the OOMe ligands (2.277–2.357 Å) and small Zr-O-O angles of about 80°. The calculated Mulliken charges at the zirconium centers prove a decrease in the Lewis acidity in the series **1a** → **1b** → **1c** → **1d** → **1e**.

To include steric effects of the bulky *tert*-butanolato and *tert*-butylperoxo ligands, the corresponding derivatives [Zr(O*t*Bu)$_4$] (**1a**$^{t\mathrm{Bu}}$) and [Zr(O*t*Bu)$_3$(OO*t*Bu)] (**1b**$^{t\mathrm{Bu}}$) were calculated (Figure 1).[12] Owing to the bulky *t*Bu units, the first exchange of a *t*BuO by a *t*BuOO ligand is endothermic ([Zr(O*t*Bu)$_4$] + *t*BuOOH → [Zr(O*t*Bu)$_3$(OO*t*Bu)] + *t*BuOH;

  0947-6539/02/0805-1050 $ 17.50+.50/0 *Chem. Eur. J.* **2002**, *8*, No. 5

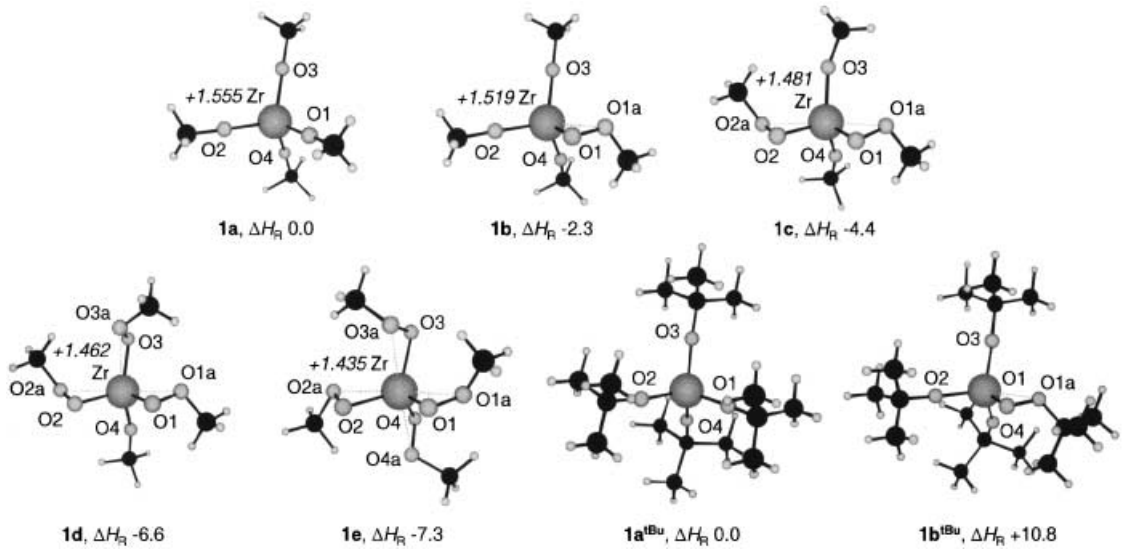

Figure 1. Calculated molecular structures and reaction enthalpies ΔH_R [kcal mol^{-1}] of compounds **1a**–**e**, **1a**^{tBu}, and **1b**^{tBu}; Mulliken charges at zirconium in italics. Selected bond lengths [Å] and angles [°]: **1a**: Zr–O1 1.951, Zr–O2 1.951, Zr–O3 1.951, Zr–O4 1.951; **1b**: Zr–O1 2.065, Zr–O2 1.942, Zr–O3 1.946, Zr–O4 1.958, Zr–O1a 2.357, O–O 1.478, Zr-O-O 81.6; **1c**: Zr–O1 2.068, Zr–O2 2.068, Zr–O3 1.955, Zr–O4 1.955, Zr–O1a 2.293; Zr–O2a 2.293, O–O_{av} 1.478, Zr-O-O_{av} 78.7; **1d**: Zr–O1 2.076, Zr–O2 2.068, Zr–O3 2.075, Zr–O4 1.939, Zr–O1a 2.300, Zr–O2a 2.277, Zr–O3a 2.349, O–O_{av} 1.478, Zr-O-O_{av} 79.2; **1e**: Zr–O1 2.075, Zr–O2 2.075, Zr–O3 2.076, Zr–O4 2.076, Zr–O1a 2.289, Zr–O2a 2.289, Zr–O3a 2.291, Zr–O4a 2.291, O–O_{av} 1.478, Zr-O-O_{av} 78.2; **1a**^{tBu}: Zr–O_{av} 1.953, Zr-O-C_{av} 176.7; **1b**^{tBu}: Zr–O1 2.069, Zr–O2 1.943, Zr–O3 1.948, Zr–O4 1.969, Zr–O1a 2.336, O–O 1.482, Zr-O-O 80.4.

ΔH_R: +10.8 kcal mol^{-1}), which still allows the monohydroperoxo species to be formed during the catalysis. The steric hindrance of the *t*BuOO ligand already forces one of *t*BuO ligands to bend away from linearity (Zr-O4-C: 157.2°). As the steric hindrance will further increase for the compounds $[Zr(OtBu)_x(OOtBu)_{4-x}]$ ($x = 2-0$), we did not calculate these species assuming that they will not play a prominent role in the real catalytic system. Therefore, $[Zr(OMe)_3(OOMe)]$ (**1b**) was used as the model system for oxygen transfer to $MeNH_2$ in the following investigations. This makes sense not only with respect to steric considerations, but also because of the decrease of Lewis acidity at zirconium, which is related to the exchange of RO by ROO (as described above, Figure 1).

Interaction of methylamine with [Zr(OMe)$_4$] (1a) and [Zr(OMe)$_3$(OOMe)] (1b): At the start of the catalytic amine oxidation, high concentrations of the substrate are present in the reaction mixture. Amines are versatile ligands, known to coordinate to zirconium alcoholates.[13] Because of the bulky substituents in the real system $[Zr(OtBu)_4]$/$[Zr(OtBu)_3(OOtBu)]$, we only included the monoamine adduct in our calculations. One equivalent of $MeNH_2$ coordinates to the model systems **1a** and **1b** in exothermic reactions (−12.3 kcal mol^{-1} and −15.8 kcal mol^{-1}, respectively) to give the corresponding trigonal-bipyramidal zirconium complexes $[Zr(OMe)_4(MeNH_2)]$ (**2a**) and $[Zr(OMe)_3(OOMe)(MeNH_2)]$ (**2b**); the amino ligand is in the axial position (Figure 2). The calculated Zr–N bond lengths (**2a**: 2.456 Å; **2b**: 2.455 Å) fit well with the data from X-ray structure analyses (2.481–2.517 Å).[13]

The isomers of **2a** and **2b** that bear the amino ligand in the equatorial position (not shown in Figure 2), were less stable than their axially substituted analogues and relaxed to the latter compounds through a Berry-type rotation during the optimization procedure. This interconversion is supported by the formation of intramolecular hydrogen bonds (N–H···OMe). The stability of the equatorial isomers of $[Zr(OtBu)_4(NH_2R)]$ and $[Zr(OtBu)_3(OOtBu)(NH_2R)]$ should be even more reduced owing to the steric demand of both the *t*Bu groups and the substituent R at the amine.

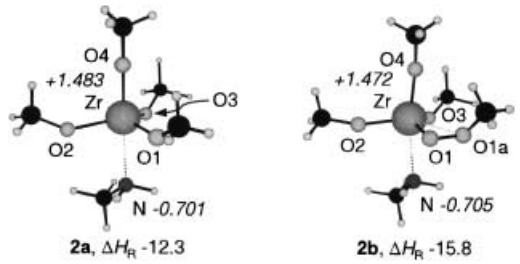

Figure 2. Calculated molecular structures and reaction enthalpies ΔH_R [kcal mol^{-1}] of the amine adducts **2a** and **2b**; Mulliken charges at zirconium and nitrogen in italics. Selected bond lengths [Å] and angles [°]: **2a**: Zr–O1 2.002, Zr–O2 1.994, Zr–O3 1.996, Zr–O4 1.959, Zr–N 2.457, O4-Zr-N 177.5; **2b**: Zr–O1 2.109, Zr–O2 1.963, Zr–O3 2.003, Zr–O4 1.963, Zr–O1a 2.389, Zr–N 2.455, O–O 1.478, Zr-O-O 81.5, O4-Zr-N 170.0.

Exchange of OR by NMeH: Since the oxygen transfer can be considered as a nucleophilic attack of the amine at HOOR or ZrOOR (see below), the decrease in the activation energy of the catalytic reaction can either result from an enhanced electrophilicity of the metal-coordinated oxygen atom or from an increased nucleophilicity of the substrate (or from a combination of both effects). Increasing the nucleophilicity of the substrate could be performed by coordinating it as an amide by the exchange of an OMe by a NHMe ligand. However, it is known that metal alcoholates are obtained by alcoholysis of appropriate amide precursors[14] as a conse-

quence of the higher acidity of alcohols compared to secondary and primary amines.[15] This is confirmed by the results of our calculations: starting from $[Zr(OMe)_4(ax\text{-}NH_2Me)]$ (**2a**) or $[Zr(OMe)_3(OOMe)(ax\text{-}NH_2Me)]$ (**2b**), aminolysis leads to $[Zr(OMe)_3(NHMe)]$ (**3a**) or $[Zr(OMe)_2(OOMe)(NHMe)]$ (*cis*-**3b**) and methanol, which is strongly endothermic by $+30.9\ kcal\,mol^{-1}$ and $+31.6\ kcal\,mol^{-1}$, respectively (Figure 3); this makes this reaction pathway quite unfavorable.

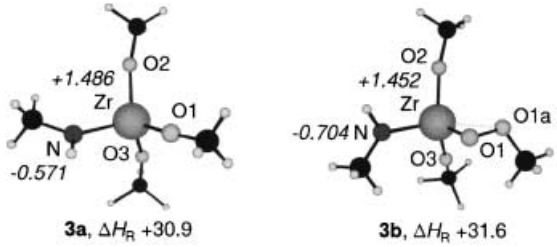

Figure 3. Calculated molecular structures and reaction enthalpies ΔH_R [kcal mol^{-1}] of the amide complexes **3a** and *cis*-**3b**, Mulliken charges at zirconium and nitrogen in italics. Selected bond lengths [Å], angles [°], and torsion angles [°]: **3a**: Zr–O1 1.953, Zr–O2 1.956, Zr–O3 1.961, Zr–N 2.065, H-N-Zr-O1 21.8; *cis*-**3b**: Zr–O1 2.061, Zr–O2 1.947, Zr–O3 1.961, Zr–O1a 2.400, Zr–N 2.058, O–O 1.480, Zr-O-O 83.6, H-N-Zr-O1 97.1.

However, there is one interesting feature of the structures shown in Figure 3: while the proton of the amido ligand in $[Zr(OMe)_3(NHMe)]$ (**3a**) is oriented almost parallel to one of the N-Zr-O planes, indicating a weak Coulomb interaction with the neighboring OMe ligand, the planar amido ligand in *cis*-**3b** is nearly perpendicular to the Zr-O-O plane. On the one hand, this prevents the formation of a hydrogen bond, but on the other hand, it allows a donor–acceptor interaction between the amido ligand (electron donor) and the methylperoxo ligand (electron acceptor). We also calculated the transition states **TS-3b**^{N1}, **TS-3b**^{N2} (rotation around the Zr–N bond) and **TS-3b**^{O} (rotation around the O–O bond) of the interconversion pathways between *cis*-**3b** and *trans*-**3b**, in which the methyl groups at the amido and the OOMe moieties have a *trans* orientation. The activation barriers ($\Delta H^{\neq} \approx 2.5\ kcal\,mol^{-1}$ relative to *cis*-**3b** and *trans*-**3b**) show that there is an almost free rotation around the Zr–N bond as well as an almost free mobility of the OOMe methyl group between two positions at ambient temperature.

To get an idea about the electronic influence of an aromatic amine and the steric influence of bulky O*t*Bu ligands of $[Zr(OtBu)_4]$ in the real catalytic system, we calculated the appropriate ligand-exchange reactions with aniline that give the anilide complexes $[Zr(OMe)_3(NHC_6H_5)]$ (**3a**^{Anil}). As expected, the ligand exchange reaction is endothermic, with a reaction enthalpy of $\approx 16.5\ kcal\,mol^{-1}$ (ΔH_R relative to **1a** and not to the amine adduct). This value is slightly lower than that calculated for the exchange of OMe against NHMe (**3a**: $+18.6\ kcal\,mol^{-1}$). This correlates with the higher acidity of aniline compared to $MeNH_2$.[15] The Zr–N bond length in **3a** is ≈ 0.05 Å shorter than the Zr–N bond length in **3a**^{Anil}.

Oxidation of methylamine to *N*-methylhydroxylamine: The primary oxygen transfer from MeOOH to $MeNH_2$ can occur at two different sites in the substrate: the oxygen may either be transferred directly to nitrogen atom by an electrophilic attack at the nitrogen lone-pair to give methylamine *N*-oxide or an insertion into a N–H bond may take place to give *N*-methyl hydroxylamine (Scheme 3).

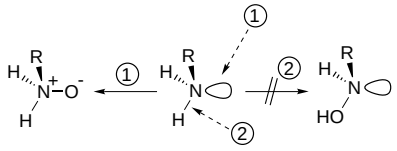

Scheme 3.

We attempted to investigate the transition states (for the catalyzed as well as for the uncatalyzed reaction) for both types; however, we did not find any indication of an insertion reaction. This does not exclude such a mode of oxygen transfer, but does indicate a higher activation barrier (compared to the N-oxidation).

During the uncatalyzed oxidation of $MeNH_2$ by MeOOH to give methylamine *N*-oxide and MeOH (electrophilic attack of the oxenoid MeO*O*H at the lone pair of the $MeNH_2$), one oxygen atom and one proton are transferred. If this pathway is considered to be a bimolecular reaction, the proton transfer is somehow related to the tautomerism of the methylhydroperoxide. Formally, this tautomerism generates methanol *O*-oxide in equilibrium, a highly reactive, electrophilic, oxygen-transfer agent, which was the subject of a recent detailed DFT study.[16] The transition state we found for the oxygen transfer, **TS1**, reflects this situation almost perfectly (Figure 4, Table 1): the nitrogen atom is attacked by the terminal oxygen atom of MeOOH, while the proton already bridges the O–O unit. This leads to an almost tetrahedral geometry around nitrogen, and the former nitrogen lone-pair interacts with the electron-deficient oxygen atom. An activation enthalpy of $+35.0\ kcal\,mol^{-1}$ was calculated for this process.

The overall reaction leading to methylamine *N*-oxide and methanol is slightly endothermic by $+0.5\ kcal\,mol^{-1}$; however, the *N*-oxide is not the final product of the first oxidation, since it tautomerizes in a strongly exothermic reaction ($-21.3\ kcal\,mol^{-1}$; relative to $MeNH_2$/MeOOH) to give *N*-methyl hydroxylamine (Figure 5). Since this tautomerization will probably not proceed exclusively by a monomolecular pathway in solution, we did not calculate its activation barrier (usually bimolecular proton transfers are rapid in protic liquid phases).

In the metal-catalyzed reaction, two different pathways, denoted by the transition states **TS1**^{Zr} and **TS1**$^{Zr'}$, are possible. The second pathway includes a preceding aminolysis reaction. Starting from the amine adduct **2b** (d(Zr–N): 2.455 Å), the transition state **TS1**^{Zr} is $+22.0\ kcal\,mol^{-1}$ higher in enthalpy (only $+6.3\ kcal\,mol^{-1}$) relative to the starting compounds (**1b**/$MeNH_2$/MeOOH). In **TS1**^{Zr}, the amine ligand is no longer coordinated to the zirconium atom (d(Zr–N): 3.242 Å), but is fixed to the catalytically active center by a NH···OMe hydrogen interaction. The oxygen transfer results in the

  0947-6539/02/0805-1052 $ 17.50+.50/0 *Chem. Eur. J.* **2002**, *8*, No. 5

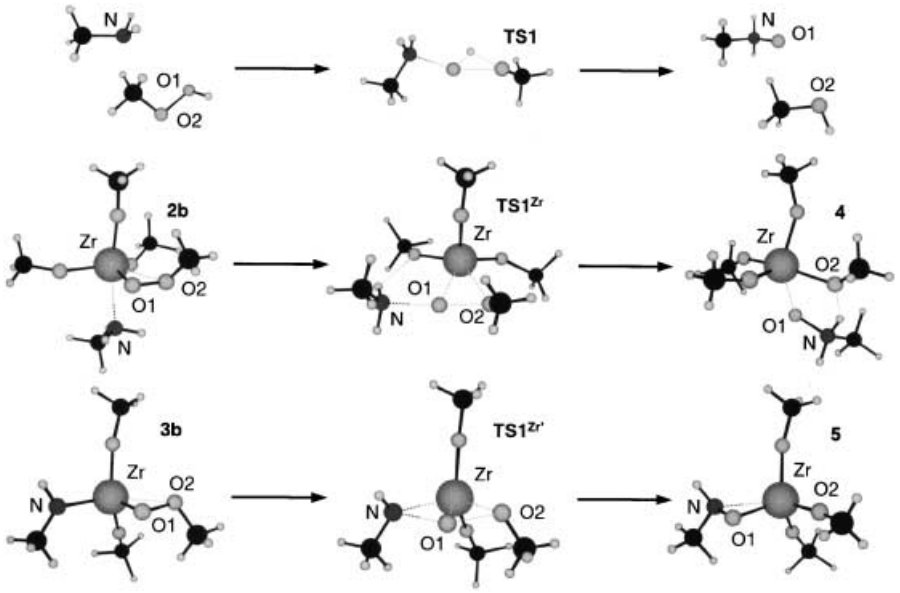

Figure 4. Calculated molecular structures of the molecules related to the transition states **TS1**, **TS1**^{Zr}, and **TS1**$^{Zr'}$.

Table 1. Calculated bond lengths [Å] and angles [°] of molecules related to the transition states **TS1**, **TS1**^{Zr}, and **TS1**$^{Zr'}$. Mulliken charges are given in italics.

	Starting compounds	Transition states	Products
	$MeNH_2$/MeOOH	**TS1**	$MeN(O)H_2$/MeOH
N–O1	–	1.851	1.354
O1–O2	1.456	1.981	–
N-O1-O2	–	160.7	–
N	*– 0.625*	*– 0.494*	*– 0.211*
O1	*– 0.412*	*– 0.436*	*– 0.548*
O2	*– 0.201*	*– 0.476*	*– 0.535*
	2a	**TS1**^{Zr}	**4**
Zr–N	2.455	3.242	3.130
Zr–O1	2.109	2.063	2.226
Zr–O2	2.389	2.201	2.132
O1–O2	1.478	1.772	2.536
N–O1	2.828	2.041	1.404
O···H	–	2.113	1.458
N-O1-O2	–	173.8	–
Zr	*+ 1.472*	*+ 1.501*	*+ 1.483*
N	*– 0.705*	*– 0.573*	*– 0.253*
O1	*– 0.438*	*– 0.381*	*– 0.520*
O2	*– 0.235*	*– 0.391*	*– 0.666*
	3a	**TS1**$^{Zr'}$	**5**
Zr–N	2.058	2.173	2.324
Zr–O1	2.061	1.943	2.063
Zr–O2	2.400	2.213	1.952
O1–O2	1.480	1.866	3.066
N–O1	3.210	2.200	1.440
N-O1-O2	–	133.9	–
Zr	*+ 1.452*	*+ 1.480*	*+ 1.493*
N	*– 0.704*	*– 0.609*	*– 0.297*
O1	*– 0.494*	*– 0.358*	*– 0.495*
O2	*– 0.219*	*– 0.407*	*– 0.558*

formation of [Zr(OMe)$_4$(*O*NH$_2$Me)] (**4**) in which the methylamine *N*-oxide coordinates to zirconium through the oxygen atom (d(Zr–O): 2.226 Å). There is also an additional NH···OMe hydrogen bond. A shift of one of the NH protons leads to the more stable tautomer [Zr(OMe)$_4$(HO*N*HMe)] (**6a**) in which the zirconium center is coordinated by the nitrogen atom (d(Zr–N): 2.519 Å) of a weakly bound *N*-methyl hydroxylamine ligand which also forms an additional OH···OMe hydrogen bond. The coordination geometry at the nitrogen atom in **TS1**^{Zr}, which closely resembles the geometry of **TS1** (tetrahedrally coordinated nitrogen, almost linear N-O-O arrangement), clearly proves that the amine acts as a nucleophile.

The pathway to the transition state **TS1**$^{Zr'}$ proceeds by a strongly endothermic preaminolysis to generate *cis*-**3b** from **2b**. The activation barrier ($\Delta H^{\neq}$) for the oxygen transfer from the methylperoxo to the resulting methylamido ligand was calculated to be +22.1 kcal mol^{-1} relative to *cis*-**3b** (+53.7 kcal mol^{-1} relative to **2b**; Figures 4 and 5). This results in an activation enthalpy of +37.9 kcal mol^{-1} relative to the starting compounds **1b**/$MeNH_2$/MeOOH, which is even more than the barrier of the uncatalyzed reaction. Because of the π donation to the metal center, the nitrogen atom in **TS1**$^{Zr'}$ is coordinated by Zr, H, and Me in an almost planar fashion. The oxenoid oxygen atom of the ZrOOMe unit attacks this π-donating orbital, which forces a coplanar orientation of the four atoms N, Zr, O, and O as well as a strong bending of the N-O-O fragment in the transition state.

After the oxygen transfer, [Zr(OMe)$_3$(MeNH*O*)] (**5**) is obtained which contains a η^2-coordinating, *N*-methylated *O*-hydroxylaminato ligand (d(Zr–O): 2.063 Å; d(Zr–N): 2.324 Å). This is the most stable molecule in this reaction sequence. The tautomer [Zr(OMe)$_3$(Me*N*OH)] (**7a**, not shown in Figure 5), which bears a η^1-coordinating, *N*-methylated *N*-hydroxylaminato ligand (d(Zr–O): 2.408 Å; d(Zr–N): 2.097 Å), was calculated to be 21.8 kcal mol^{-1} higher in enthalpy than **5**. These results suggest that the catalyzed oxygen transfer to $MeNH_2$ should *not* proceed via a coordinated amide, mainly as a consequence of the energetically unfavorable formation of the amide precursor.

Oxidation of *N*-methylhydroxylamine to nitrosomethane: Analogously to the first oxidation of methylamine (see above), the second oxygen atom can be formally transferred either to the nitrogen atom of *N*-methyl hydroxylamine to give *N*-methyl hydroxylamine *N*-oxide or inserted into the N–H bond of the substrate to yield *N*-methyl dihydroxylamine (Scheme 4). Again, we could not find any indication of the insertion reaction.

The uncatalyzed oxidation of MeNH(OH) (Figure 6, Table 2) proceeds via the transition state **TS2**, which closely resembles the transition state **TS1** of the oxygen transfer to $MeNH_2$ (parallel oxygen and proton transfer; see Figure 4). Again, the tetrahedral coordination of the nitrogen atom

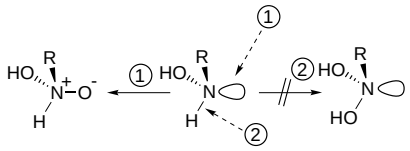

Scheme 4.

proves the nucleophilic attack at the terminal oxygen atom of MeOOH.

An activation enthalpy of $+31.1$ kcal mol^{-1} was calculated for **TS2**, which is ≈ 3.8 kcal mol^{-1} lower than the barrier related to **TS1**. This may be caused by a stabilizing interaction of the OH proton of MeNH(OH) with the HO oxygen atom of the oxidizing agent (d(OH$\cdots$O): 2.077 Å; bond angle(O–H$\cdots$O): 104.3°), which slightly reduces the N$\cdots$O distance in **TS2** relative to that found in to **TS1** (**TS2**, d(N$\cdots$O): 1.847 Å; **TS1**, d(N$\cdots$1.851 Å). Again, the *N*-oxide is only an intermediate of the oxidation. In a first exothermic step, it tautomerizes to *N*-methyl dihydroxylamine ($CH_3NH(O)OH \rightarrow CH_3N(OH)_2$, ΔH_R: -10.7 kcal mol^{-1}), which then eliminates water to give nitrosomethane ($CH_3N(OH)_2 \rightarrow CH_3NO + H_2O$, ΔH_R: -6.3 kcal mol^{-1}). The overall reaction from *N*-methyl hydroxylamine to nitrosomethane is exothermic by -36.0 kcal mol^{-1} (Figure 7).

As mentioned for the first zirconium-catalyzed oxygen-transfer step, there are also two different pathways for the second oxygen transfer; they are related to two transition states **TS2**^{Zr} and **TS2**$^{Zr'}$. The hydroxyl amine adduct **6a** (Figure 5), which is the most stable intermediate in the first oxidation sequence, can either undergo a ligand exchange (OMe vs. OOMe) to yield the hexacoordinate complex **6b**, or perform a hydroxylaminolysis to give complex **7a**, which then is transformed into the corresponding hexacoordinate complex **7b** (N-oxidation of a coordinated hydroxylamido ligand requires the OH and not the NH tautomer).

Following the first sequence and starting from **1a**/MeNH(OH)/MeOOH, results in **TS2**^{Zr}, with an activation enthalpy of $+1.2$ kcal mol^{-1} (relative to **1a** + MeNH(OH) + MeOOH $\rightarrow$ **TS2**^{Zr} + MeOOH; $+18.3$ kcal mol^{-1} relative to **6b** $\rightarrow$ **TS2**^{Zr}). This is far below the barrier of the uncatalyzed reaction ($+31.1$ kcal mol^{-1}). The MeNH(OH) ligand is decoordinated from the zirconium center (d(Zr–N): 3.375 Å) as

Table 2. Calculated bond lengths [Å] and angles [°] of molecules related to the transition states **TS2**, **TS2**^{Zr} and **TS2**$^{Zr'}$. Mulliken charges are given in italics.

	Starting compounds	Transition states	Products
	MeNH(OH)/MeOOH	**TS2**	MeNH(O)OH/MeOH
N–O1	1.450	1.404	1.536
N–O2	–	1.847	1.291
O2–O3	1.456	1.971	–
N-O2-O3	–	162.4	–
N	*−0.264*	*−0.106*	*−0.089*
O1	*−0.517*	*−0.473*	*−0.536*
O2	*−0.412*	*−0.474*	*−0.463*
O3	*−0.201*	*−0.469*	*−0.535*
	6b	**TS2**^{Zr}	**8**
Zr–N	2.535	3.375	3.292
Zr–O2	2.077	2.064	2.273
Zr–O3	2.461	2.194	1.977
O2–O3	1.469	1.774	3.102
N–O1	1.432	1.417	1.422
N–O2	2.693	2.048	1.361
O$\cdots$H	1.707	1.692	1.451
N-O2-O3	–	178.7	–
Zr	*+1.482*	*+1.530*	*+1.506*
N	*−0.316*	*−0.174*	*−0.087*
O1	*−0.517*	*−0.526*	*−0.508*
O2	*−0.446*	*−0.407*	*−0.503*
O3	*−0.194*	*−0.388*	*−0.575*
	7b	**TS2**$^{Zr'}$	**9**
Zr–N	2.110	2.183	2.860
Zr–O1	2.319	3.075	2.490
Zr–O2	2.071	1.921	2.068
Zr–O3	2.304	2.216	1.939
O2–O3	1.477	1.928	3.079
N–O1	1.513	1.404	1.503
N–O2	2.950	2.547	1.401
N-O2-O3	–	126.4	–
Zr	*+1.443*	*+1.432*	*+1.464*
N	*−0.309*	*−0.216*	*−0.134*
O1	*−0.533*	*−0.441*	*−0.537*
O2	*−0.400*	*−0.393*	*−0.521*
O3	*−0.232*	*−0.395*	*−0.553*

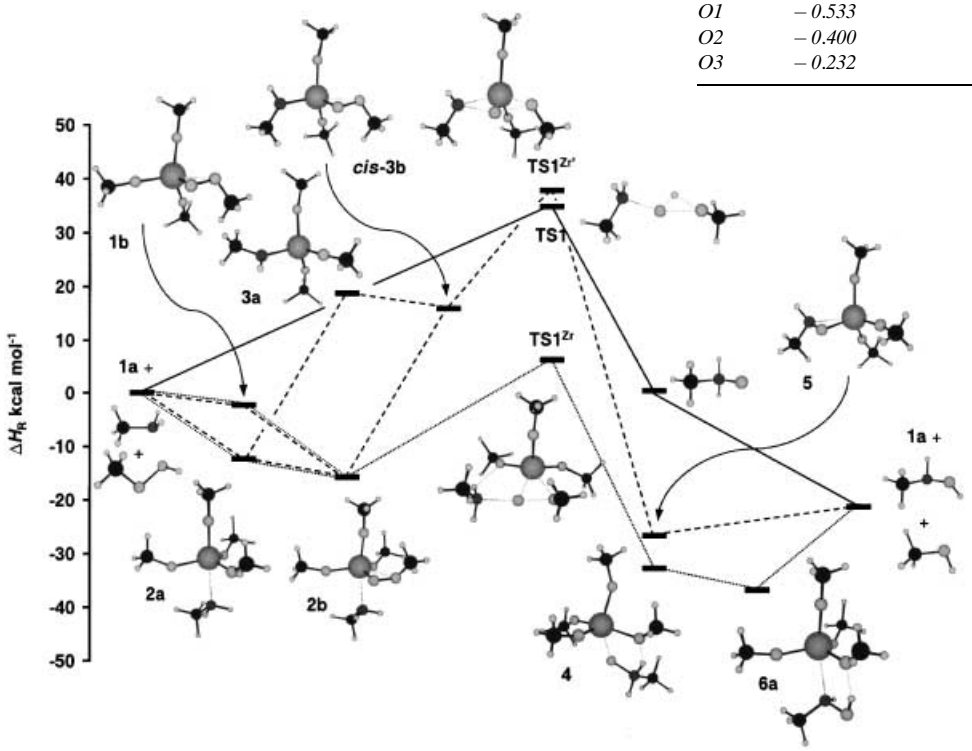

Figure 5. Calculated pathways for the oxidation of $MeNH_2$ to MeNH(OH); —— uncatalyzed reaction, •••• catalyzed reaction without zirconium amide intermediate, ---- catalyzed reaction with zirconium amide intermediate.

0947-6539/02/0805-1054 $ 17.50+.50/0 *Chem. Eur. J.* **2002**, *8*, No. 5

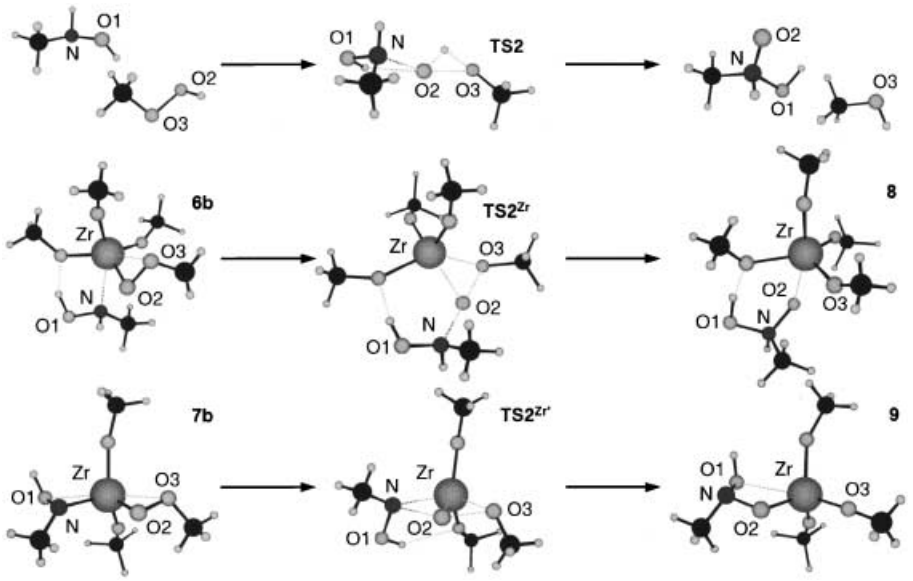

Figure 6. Calculated molecular structures related to the transition states **TS2**, **TS2**^{Zr}, and **TS2**$^{Zr'}$. Mulliken charges in italics.

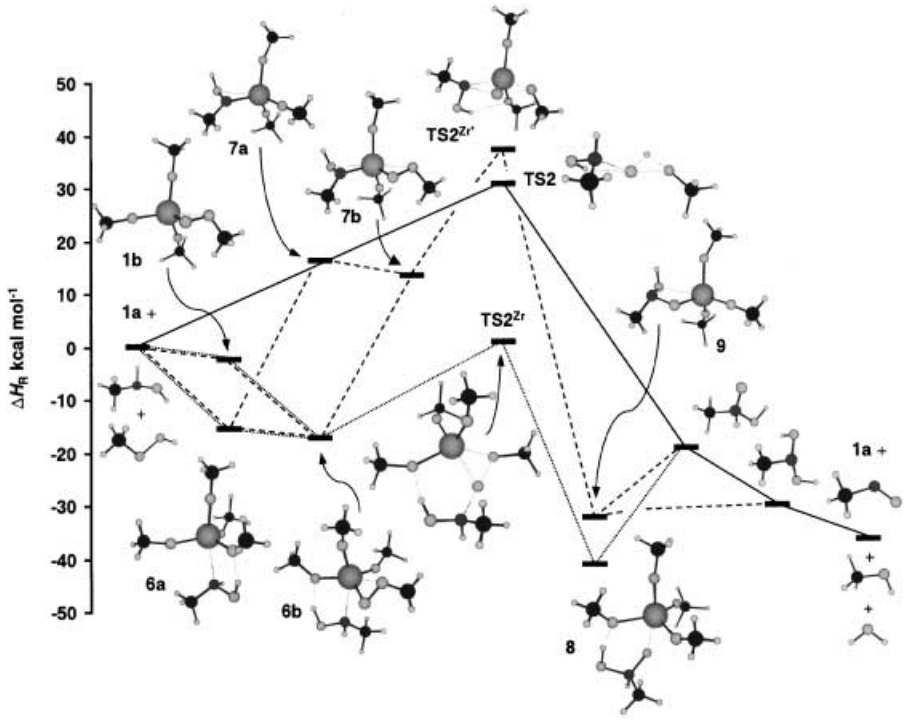

Figure 7. Calculated pathways for the oxidation of MeNH(OH) to MeNO; —— uncatalyzed reaction, •••• catalyzed reaction without zirconium amide intermediate, ---- catalyzed reaction with zirconium amide intermediate.

was the $MeNH_2$ fragment in **TS1**^{Zr}, but stays connected to the catalyst through a hydrogen bond between the OH group of MeNH(OH) and one of the methanolato ligands (d(N–OH···OMe): 1.692 Å; bond angle(O–H···O): 168.6°). The oxygen transfer finally yields the pentacoordinate complex **8**, an adduct of *N*-methyl hydroxylamine *N*-oxide (MeNH(O)(OH)) to **1a**, in which the *N*-oxide unit coordinates to zirconium (d(Zr–O): 2.273 Å). This is supported by a hydrogen bond between the OH group of MeNH(O)(OH) and one of the OMe ligands on zirconium (d(N–OH···OMe): 1.451 Å; bond angle(O–H···O): 168.7°). Splitting off MeNH(O)(OH), tautomerization, and dehydration will give nitrosomethane, as described for the uncatalyzed reaction. The geometry of **TS2**^{Zr} agrees with the postulation of an electrophilic attack at the nitrogen atom.

TS2$^{Zr'}$, which closely resembles the transition state **TS1**$^{Zr'}$, can only be reached by means of a strongly endothermic hydroxylaminolysis which generates **7b** from **6b** (Figure 7; ΔH_R: +30.8 kcal mol^{-1}). The calculated activation enthalpy is +23.8 kcal mol^{-1} relative to **7b** → **TS2**$^{Zr'}$ and +37.5 kcal mol^{-1} relative to **1a** + MeNHOH + MeOOH → **TS2**$^{Zr'}$ + MeOH, respectively. The reaction product of this pathway is the pentacoordinate compound **9**, which bears a monodeprotonated *N*-methyl dihydroxylamino ligand, η^2-coordinated to zirconium by two oxygen atoms (d(Zr–O1): 2.068 Å; d(Zr–O2): 2.490 Å). Ligand exchange of [MeN(OH)O]$^-$ by MeO$^-$ will regenerate **1a** and liberate *N*-methyl dihydroxylamine (MeN(OH)$_2$) or *N*-methyl hydroxylamine *N*-oxide (MeNH(O)(OH)), which will then loose water to yield MeNO.

As a result of these calculations it is clear that the second oxygen transfer does not require a zirconium-coordinated amide (**TS2**$^{Zr'}$) as has already been demonstrated for the first oxygen-transfer step. The oxygen atom is transferred directly to a noncoordinated *N*-methyl hydroxylamine molecule.

Oxidation of nitrosomethane to nitromethane: In contrast to the first and second oxidation, there is only one single site for the third oxygen-transfer step: the nitrogen atom. The uncatalyzed reaction proceeds via the transition state **TS3**, with an activation enthalpy of 24.0 kcal mol^{-1} (Figure 8, Table 3), which is 7.1 kcal mol^{-1} lower in energy than the barrier related to **TS2**. The reaction $CH_3NO + CH_3OOH \rightarrow CH_3NO_2 + CH_3OH$ was found to be strongly exothermic (ΔH_R: −51.7 kcal mol^{-1}).

However, while $MeNH_2$/MeNH(OH) are negatively polarized substrates (Mulliken charges: −0.625 and −0.264 at nitrogen), the nitrogen atom of MeNO carries a positive charge (+0.077). This means that this compound will no longer act as a nucleophile but as an electrophile. Therefore,

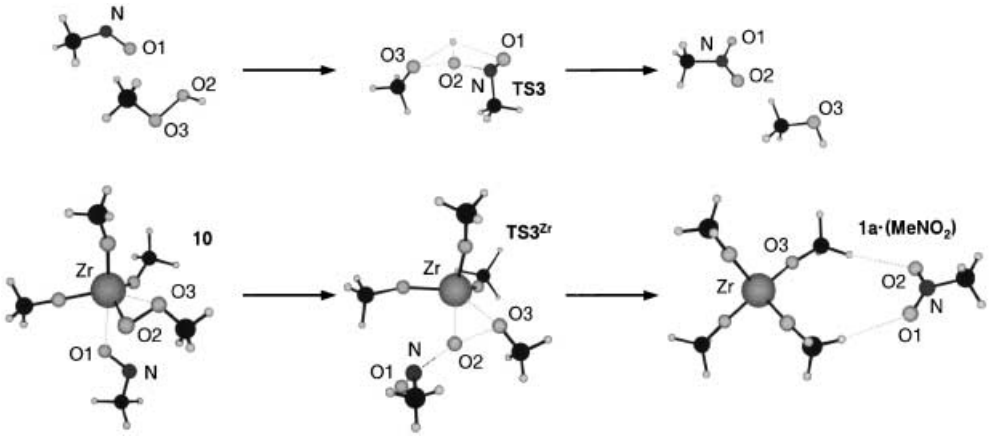

Figure 8. Calculated molecular of molecules related to the transition states **TS3** and **TS3**^{Zr}.

Table 3. Calculated bond lengths [Å] and angles [°] of molecules related to the transition states **TS3** and **TS3**^{Zr}. Mulliken charges are given in italics.

	Starting compounds	Transition states	Products
	MeNO/MeOOH	**TS3**	$MeNO_2$/MeOH
N–O1	1.219	1.229	1.234
N–O2	–	1.608	1.234
O2–O3	1.456	1.864	–
N-O2-O3	–	145.9	–
N	*+0.077*	*+0.183*	*+0.367*
O1	*−0.196*	*−0.253*	*−0.277*
O2	*−0.412*	*−0.373*	*−0.277*
O3	*−0.201*	*−0.343*	*−0.535*
	10	**TS3**^{Zr}	**1a**·($MeNO_2$)
Zr–O1	2.690	–	–
Zr–O2	2.075	2.122	–
Zr–O3	2.384	2.219	–
O2–O3	1.477	1.764	–
N–O1	1.220	1.212	1.234
N–O2	3.398	1.827	1.234
N-O2-O3	–	164.7	–
O1···H	–	–	2.665, 2.692
Zr	*+1.446*	*+1.553*	*+1.545*
N	*+0.143*	*+0.210*	*+0.378*
O1	*−0.167*	*−0.189*	*−0.277*
O2	*−0.432*	*−0.434*	*−0.280*
O3	*−0.215*	*−0.368*	*−0.569*

the geometry at nitrogen in **TS3** is trigonal-pyramidal (sum of bond angles: 341.2°) with the free electron pair not mainly interacting with the oxidizing agent. Additionally, the OH proton of MeOOH in **TS3** is not mainly bridging the O–O unit as it did in **TS1**/**TS2** (bond angle O-O-H: 43.4° and 44.8°). It is located in a position for which its function can be interpreted as a combination of bridging the O–O fragment (bond angle O-O-H: 83.2°) and forming a weak H bridge to the MeNO oxygen atom (dihedral angle H–O···N–O: 31.7°; distance O–H···O–N: 2.423 Å). The bending of the N-O-O unit (145.7°) is more pronounced than in **TS1** and **TS2**.

Nitrosomethane is also directly oxidized during the zirconium-catalyzed reaction. Its coordination to [$Zr(OMe)_3$(OOMe)] is only weak ([$Zr(OMe)_3$(OOMe)] + CH_3NO → $OMe)_3$(OOMe)(CH_3NO); ΔH_f: −3.9 kcal mol^{-1}); only coordination by the oxygen atom gives a stable intermediate. We found a barrier ($\Delta H^{\neq}$) for the oxygen transfer (**TS3**^{Zr}) of only +8.6 kcal mol^{-1} for the reaction starting from [$Zr(OMe)_3$(OOMe)(CH_3NO)] (**10**), which is only +4.7 kcal mol^{-1} relative to the starting materials. This implies that nitroso derivatives should generally be oxidized rapidly to the corresponding nitro compounds and agrees with the observation that the isolation of nitroso compounds from a catalytic reaction mixture requires special conditions.[4] Additionally, the difference between the activation barriers of the uncatalyzed and the catalyzed reaction has become smaller. This agrees with the observation that electron-poor nitroso derivatives can be oxidized without a catalyst to give the corresponding nitro compounds. The donor potential of the final product CH_3NO_2 is even weaker than that of CH_3NO, which prevents the formation of a stable adduct to the zirconium center. Optimization of the system [$Zr(OMe)_4$]/CH_3NO_2 gives complex **1a**·($MeNO_2$) in which the nitro group is very weakly bonded to two hydrogen atoms of two OMe ligands (ΔH_R: −1.4 kcal mol^{-1}). This complex should evidently dissociate immediately in solution. Figure 9 gives an overview of the two pathways of the MeNO oxidation.

Conclusion

Figure 10 presents a graphical summary of our investigations. The stepwise oxidation of amines in the presence of zirconium alkoxides is energetically favored in all three steps compared to the metal-free procedure. A formation of intermediate zirconium amides is not required in the catalyzed sequences.

Owing to a subsequent lost of electron density parallel to the oxidation of the nitrogen atom, a switch in the oxygen-transfer mechanism takes place: $MeNH_2$ and MeNH(OH) are oxidized by an electrophilic attack of the hydroperoxide (MeOOH or ZrOOH), while for MeNO, a nucleophilic attack was proved. This confirms with experimental data of amine oxidations.

Experimental Section

Methods: Quantum chemical calculations were performed with the program Gaussian 98W[17] and the B3LYP gradient-corrected exchange-correlation functional[18] in combination with the Los Alamos effective-core potentials on zirconium atoms together with a Gaussian valence basis

0947-6539/02/0805-1056 $ 17.50+.50/0 *Chem. Eur. J.* **2002**, *8*, No. 5

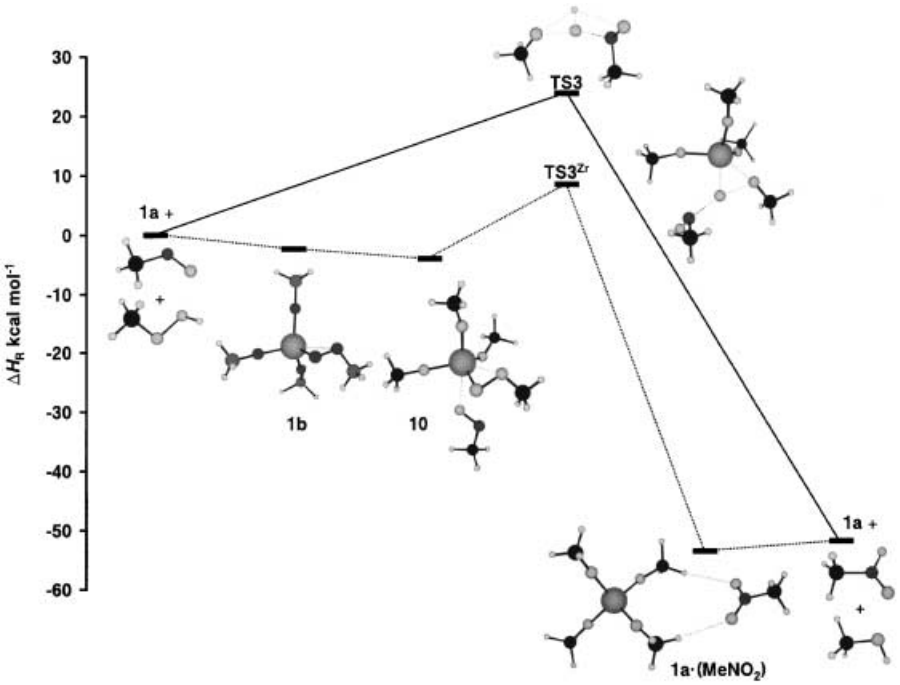

Figure 9. Calculated pathways for the oxidation of MeNO to $MeNO_2$; —— uncatalyzed reaction, •••• catalyzed reaction.

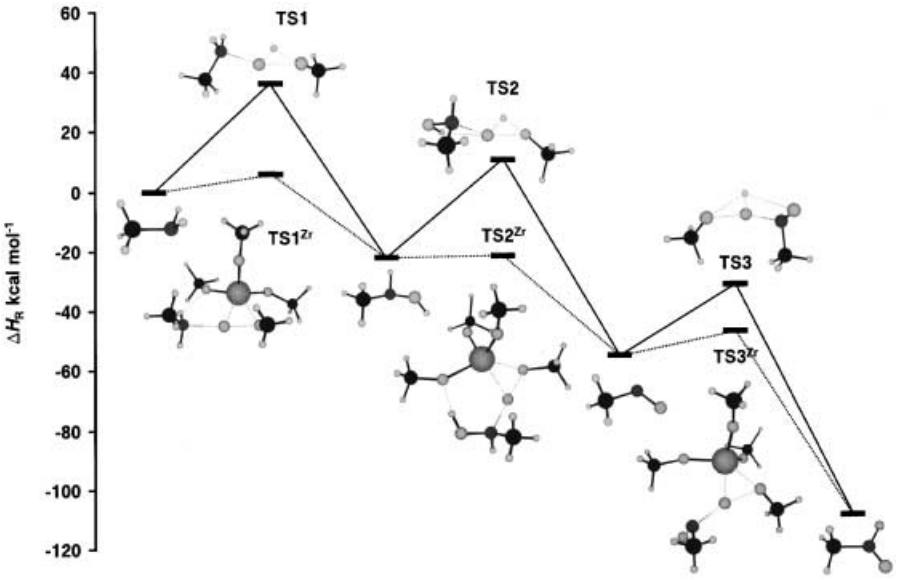

Figure 10. Comparison of the uncatalyzed and catalyzed oxidation of $MeNH_2$ to $MeNO_2$.

set of double zeta quality (LanL2DZ).[19] The orbital basis sets of carbon, nitrogen, and oxygen atoms were augmented by a single set of polarization functions.[20] Full geometry optimizations were carried out in C_1 symmetry with analytical gradient techniques, and the resulting structures were confirmed to be true minima or transition states by diagonalization of the analytical Hessian Matrix. The reaction enthalpies and the activation enthalpies given are corrected to a temperature of 298.150 K and a pressure of 1.000 atm.

Acknowledgement

We wish to thank the Deutsche Forschungsgemeinschaft (Schwerpunktprogramm "Peroxidchemie") and the Fonds der Chemischen Industrie for financial support.

[1] Review: H. Adam, K. Khanbabaee, K. Krohn, J. Küpke, H. Rieger, K. Steingröver, I. Vinke, *Transition-Metal Alkoxide-Catalyzed Oxidation of Phenols, Alcohols, and Amines with tert-Butyl Hydroperoxide* in *Peroxide Chemistry, Mechanistic and Preparative Aspects of Oxygen Transfer* (Ed.: W. Adam), Wiley-VCH, Weinheim **2000**, pp. 469–493.

[2] K. Krohn, J. Küpke, H. Rieger, *J. Prakt. Chem.* **1997**, *339*, 335–339.

[3] T. L. Gilchrist, *Comprehensive Organic Transformations*, *Vol. 7*, (Eds.: B. M. Trost, I. Fleming) Pergamon Press, Oxford **1991**, pp. 736–737.

[4] K. Krohn, J. Küpke, *Eur. J. Org. Chem.* **1998**, 679–682.

[5] K. E. Gilbert, W. T. Borden, *J. Org. Chem.* **1979**, *44*, 659–661.

[6] K Krohn, K. Steingröver, *J. Prakt. Chem.* **2000**, *342*, 192–194.

[7] K. Krohn, J. Küpke, *J. Prakt. Chem.* **1999**, 509–511.

[8] a) G. Boche, F. Bosold, J. C. W. Lohrenz, *Angew. Chem.* **1994**, *106*, 1228–1230; *Angew. Chem. Int. Ed. Engl.* **1994**, *33*, 1161–1163; b) R. D. Bach, M.-D. Su, J. L. Andrés, H. B. Schlegel, *J. Am. Chem. Soc.* **1993**, *115*, 8763–8769; c) G. Boche, K. Möbus, K. Harms, J. C. W. Lohrenz, M. Marsch, *Chem. Eur. J.* **1996**, *2*, 604–607; d) G. Boche, K. Möbus, K. Harms, M. Marsch, *J. Am. Chem. Soc.* **1996**, *118*, 2770–2771; e) Y.-D. Wu, D. K. W. Lai, *J. Am. Chem. Soc.* **1995**, *117*, 11327–11336; f) Y.-D. Wu, D. K. W. Lai, *J. Org. Chem.* **1995**, *60*, 673–680; g) G. Boche, J. C. W. Lohrenz, *Chem. Rev.* **2001**, *101*, 697–756.

[9] a) W. R. Thiel, T. Priermeier, *Angew. Chem.* **1995**, *107*, 1870–1871; *Angew. Chem. Int. Ed. Engl.* **1995**, *34*, 1737–1738; b) W. R. Thiel, *Chem. Ber.* **1996**, *129*, 575–580; c) W. R. Thiel, J. Eppinger, *Chem. Eur. J.* **1997**, *3*, 696–705; d) H. Glas, M. Spiegler, W. R. Thiel, *Eur. J. Inorg. Chem.* **1998**, 275–281; e) A. Hroch, G. Gemmecker, W. R. Thiel, *Eur. J. Inorg. Chem.* **2000**, 1107–1114; f) W. R. Thiel, M. Barz, H. Glas, A.-K. Pleier, *Olefin Epoxidation Catalyzed by Molybdenum Peroxo Complexes: A Mechanistic Study* in *Peroxide Chemistry: Mechanistic and Preparative Aspects of Oxygen Transfer* (Ed.: W. Adam), Wiley-VCH, **2000**, pp. 433–453.

[10] J. A. Samuels, E. B. Lobkovsky, W. E. Streib, K. Folting, J. C. Huffman, J. W. Zwanziger, K. G. Caulton, *J. Am. Chem. Soc.* **1993**, *115*, 5093–5104.

[11] a) B. A. Vaartstra, J. C. Huffman, P. S. Gradeff, L. G. Hubert-Pfalzgraf, J.-C. Daran, S. Parraud, K. Yunlu, K. G. Caulton, *Inorg. Chem.* **1990**, *29*, 3126–3131; b) T. J. Boyle, R. W. Schwartz, R. J. Doedens, J. W. Ziller, *Inorg. Chem.* **1995**, *34*, 1110–1120; c) W. J. Evans, M. A. Ansari, J. W. Ziller, *Inorg. Chem.* **1999**, *38*, 1160–1164; d) Z. A. Starikova, E. P. Turevskaya, N. I. Kozlova, N. Y. Turova, D. V. Berdyev, A. I. Yanovsky, *Polyhedron* **1999**, *18*, 941–947; e) G.

Kickelbick, U. Schubert, *J. Chem. Soc. Dalton. Trans.* **1999**, 1301 – 1305.
[12] Owing to the flat PES, the geometry optimization of [Zr(O*t*Bu)$_4$] (**1a**^{tBu}) and [Zr(O*t*Bu)3(OO*t*Bu)] (**1b**^{tBu}) was stopped before all four convergence criteria of GAUSSIAN were reached. However, the maximum force and the RMS force were far below the cutoff values and the energy differences between two succeeding optimization steps were below 10^{-3} kcal mol^{-1}.
[13] K. A. Fleeting, P. O'Brian, A. C. Jones, D. J. Otway, A. J. P. Andrew, D. J. Williams, *J. Chem. Soc. Dalton Trans.* **1999**, 2853 – 2859.
[14] I. M. Thomas, *Can. J. Chem.* **1961**, *39*, 1386- 1388.
[15] a) J. March, *Advanced Organic Chemistry*, 4th ed., Wiley, New York **1992**, pp. 250 – 252; b) *Organikum*, 20th ed., Barth, Heidelberg **1996**, p. 156.
[16] C. A. Schalley, J. N. Harvey, D. Schröder, H. Schwarz, *J. Phys. Chem. A* **1998**, *102*, 1021 – 1035.
[17] M. J. Frisch, G. W. Trucks, H. B. Schlegel, G. E. Scuseria, M. A. Robb, J. R. Cheeseman, V. G. Zakrzewski, J. A. Montgomery, Jr., R. E. Stratmann, J. C. Burant, S. Dapprich, J. M. Millam, A. D. Daniels, K. N. Kudin, M. C. Strain, O. Farkas, J. Tomasi, V. Barone, M. Cossi, R. Cammi, B. Mennucci, C. Pomelli, C. Adamo, S. Clifford, J. Ochterski, G. A. Petersson, P. Y. Ayala, Q. Cui, K. Morokuma, D. K. Malick, A. D. Rabuck, K. Raghavachari, J. B. Foresman, J. Cioslowski, J. V. Ortiz, A. G. Baboul, B. B. Stefanov, G. Liu, A. Liashenko, P. Piskorz, I. Komaromi, R. Gomperts, R. L. Martin, D. J. Fox, T. Keith, M. A. Al-Laham, C. Y. Peng, A. Nanayakkara, C. Gonzalez, M. Challacombe, P. M. W. Gill, B. G. Johnson, W. Chen, M. W. Wong, J. L. Andres, M. Head-Gordon, E. S. Replogle, J. A. Pople, Gaussian 98 (Revision A.7), Gaussian, Inc., Pittsburgh PA, **1998**.
[18] a) C. Lee, W. Yang, R. G. Parr, *Phys. Rev. B* **1988**, *37*, 785 – 789; b) A. D. Becke, *Phys. Rev. A* **1988**, *38*, 3098 – 3100; c) B. Miehlich, A. Savin, H. Stoll, H. Preuss, *Chem. Phys. Lett.* **1989**, *157*, 200 – 206.
[19] a) J. B. Foresman, T. A. Keith, K. B. Wiberg, J. Snoonian, M. J. Frisch, *J. Phys. Chem.* **1996**, *100*, 16098 – 16104; b) W. J. Stevens, H. Basch, J. Krauss, *J. Chem. Phys.* **1984**, *81*, 6026 – 6033; c) W. J. Stevens, M. Krauss, H. Basch, P. G. Jasien, *Can. J. Chem.* **1992**, *70*, 612 – 630; d) T. R. Cundari, W. J. Stevens, *J. Chem. Phys.* **1993**, *98*, 5555 – 5565.
[20] P. C. Hariharan, J. A. Pople, *Theoret. Chimica Acta* **1973**, *28*, 213 – 222.

Received: June 6, 2001 [F3318]

  0947-6539/02/0805-1058 $ 17.50+.50/0